



## King's Research Portal

DOI:

[10.1097/MNM.0000000000000849](https://doi.org/10.1097/MNM.0000000000000849)

*Document Version*

Publisher's PDF, also known as Version of record

[Link to publication record in King's Research Portal](#)

*Citation for published version (APA):*

Lu, Z., Xie, J., Yan, R., Yu, Z., Sun, Z., Yu, F., Gong, X., Feng, H., Lu, J., & Zhang, Y. (2018). A pilot study of pancreatic islet amyloid PET imaging with [<sup>18</sup>F]FDDNP. *Nuclear Medicine Communications*, 39(7), 659-664. <https://doi.org/10.1097/MNM.0000000000000849>

### **Citing this paper**

Please note that where the full-text provided on King's Research Portal is the Author Accepted Manuscript or Post-Print version this may differ from the final Published version. If citing, it is advised that you check and use the publisher's definitive version for pagination, volume/issue, and date of publication details. And where the final published version is provided on the Research Portal, if citing you are again advised to check the publisher's website for any subsequent corrections.

### **General rights**

Copyright and moral rights for the publications made accessible in the Research Portal are retained by the authors and/or other copyright owners and it is a condition of accessing publications that users recognize and abide by the legal requirements associated with these rights.

- Users may download and print one copy of any publication from the Research Portal for the purpose of private study or research.
- You may not further distribute the material or use it for any profit-making activity or commercial gain
- You may freely distribute the URL identifying the publication in the Research Portal

### **Take down policy**

If you believe that this document breaches copyright please contact [librarypure@kcl.ac.uk](mailto:librarypure@kcl.ac.uk) providing details, and we will remove access to the work immediately and investigate your claim.

## Original article

# A pilot study of pancreatic islet amyloid PET imaging with [<sup>18</sup>F]FDDNP

Zhi Lu<sup>a,\*</sup>, Jinghui Xie<sup>a,\*</sup>, Ran Yan<sup>c,\*</sup>, Zilin Yu<sup>c</sup>, Zhigang Sun<sup>b</sup>, Fei Yu<sup>a</sup>, Xiaoyan Gong<sup>a</sup>, Hongbo Feng<sup>a</sup>, Jing Lu<sup>a</sup> and Yanjun Zhang<sup>a</sup>

**Objectives** Pancreatic islet amyloid deposition occurs before  $\beta$ -cell damage in type 2 diabetes mellitus patients. The islet and Alzheimer's disease  $\beta$ -amyloid shares similar secondary structures. The Alzheimer's disease  $\beta$ -amyloid targeting tracer [<sup>18</sup>F]FDDNP could be used to image pancreatic islet amyloid with PET.

**Patients and methods** Consecutive pancreatic tissue sections from a 69-year-old male type 2 diabetes mellitus patient were stained by hematoxylin and eosin, anti-amylin antibody, Congo Red, periodic acid-Schiff, and [<sup>18</sup>F]FDDNP reference compound, respectively. The pancreatic tissue sections were also incubated with [<sup>18</sup>F]FDDNP with and without its reference compound for autoradiography. Subsequently, we performed control [<sup>18</sup>F]FDDNP pancreatic PET/CT imaging in four healthy individuals. The mean standardized uptake values of [<sup>18</sup>F]FDDNP uptake in the pancreatic head, neck, body, and tail, blood pool, liver, and vertebral bone from 5 to 120 min after injection were determined.

**Results** Islet amyloid was observed in all four standard staining methods in the pancreas tissue. Similar islet amyloid distribution and phenotypes were observed clearly in the [<sup>18</sup>F]FDDNP reference compound-stained pancreas tissue. [<sup>18</sup>F]FDDNP was intensively accumulated in the same pancreatic tissue in autoradiography, which was

largely blocked by its reference compound. In the PET/CT scans of control human participants, the mean standardized uptake values in pancreas decreased to the blood pool level in 30 min and all parts of the pancreas had similar [<sup>18</sup>F]FDDNP uptake. The pancreas could be distinguished clearly from the liver at all-time points.

**Conclusion** These results suggested that [<sup>18</sup>F]FDDNP is a potential tracer for pancreatic islet amyloid PET imaging. *Nucl Med Commun* 00:000–000 Copyright © 2018 The Author(s). Published by Wolters Kluwer Health, Inc.

Nuclear Medicine Communications 2018, 00:000–000

**Keywords:** diabetes, [<sup>18</sup>F]FDDNP, human islet amyloid, PET

Departments of <sup>a</sup>Nuclear Medicine, <sup>b</sup>Pathology, the First Affiliated Hospital of Dalian Medical University, Dalian, People's Republic of China and <sup>c</sup>Department of Imaging Chemistry and Biology, School of Biomedical Engineering and Imaging Sciences, King's College London, King's Health Partners, St Thomas' Hospital, London, UK

Correspondence to Yanjun Zhang, MD, Department of Nuclear Medicine, the First Affiliated Hospital of Dalian Medical University, No.222 Zhongshan Road, Dalian, Liaoning 116011, People's Republic of China  
Tel: +86 411 8363 5963 x2319; fax: +86 411 8439 4205;  
e-mail: yjzhang78@163.com

\*Zhi Lu, Jinghui Xie and Ran Yan contributed equally to the writing of this article.

Received 9 December 2017 Revised 19 March 2018 Accepted 1 April 2018

## Introduction

Diabetes is a chronic progressive disease characterized by elevated levels of blood glucose. The prevalence of diabetes has been increasing steadily for the past three decades and is growing most rapidly in low-income and middle-income countries. Diabetes caused 1.5 million deaths in 2012. In 2014, 422 million individuals in the world had diabetes, a prevalence of 8.5% among the adult population [1].

Type 2 diabetes mellitus (T2DM) accounts for the vast majority of diabetes patients, and is characterized by islet  $\beta$ -cell damage and dysfunction. Amyloid deposits can be

found in the pancreatic islets around  $\beta$  cells in over 90% of T2DM patients [2,3]. Human islet amyloid polypeptide is a 37-residue amyloidogenic peptide hormone secreted primarily by pancreatic  $\beta$  cells in the islet of Langerhans simultaneously with insulin [4]. In-vitro studies have suggested that the human islet amyloid polypeptide has a concentration-dependent amyloidogenic propensity that causes cell membrane disruption, channel formation, and cytotoxicity. The resulting insoluble plaques have the characteristic  $\beta$ -sheet structure of amyloidogenic proteins [5]. Furthermore, islet amyloidosis occurs uniformly throughout the pancreas, affecting all islets before severely damaging their functions. Reduction of islet endocrine mass also occurs at this early stage of islet amyloid development and progresses as the amyloid mass increases [6]. In a study on monkeys, glucose tolerance deteriorated as the amount of islet amyloid increased [7]. In addition, islet amyloidosis appears to be associated with a reduction in islet  $\beta$ -cell mass, especially

The data were presented previously at the SNMMI 2015 Annual Meeting and published as an abstract in *J Nucl Med* 2015; **56**:1067.

This is an open-access article distributed under the terms of the Creative Commons Attribution-Non Commercial-No Derivatives License 4.0 (CCBY-NC-ND), where it is permissible to download and share the work provided it is properly cited. The work cannot be changed in any way or used commercially without permission from the journal.

when marked islet amyloid is present [8,9]. These researches indicate that amyloid deposition occurs before  $\beta$ -cell damage in pancreatic islets and consequently the symptom of high blood glucose levels appears.

Currently, the only clinical method to diagnose pancreatic islet amyloid is through invasive autopsy. Thus, there is an unmet need to develop a noninvasive imaging method to quantitatively measure the pancreatic islet amyloid burden in T2DM patients. So far, only one molecular probe,  $^{99m}\text{Tc}$ -labeled pyridyl benzofuran, has been evaluated *in vivo* on the islet amyloid mouse model with single-photon emission computed tomography [10]. It showed a 1.6-fold higher uptake in the pancreas of the model mice than the control mice at 1 h after injection. Recently, [ $^{18}\text{F}$ ]FDDNP has shown great promise in the detection of  $\beta$ -amyloid burden in Alzheimer's diseases (AD) patients [11,12]. As the islet and AD  $\beta$ -amyloid has a similar secondary structure [13], we envisage that [ $^{18}\text{F}$ ]FDDNP could be applied for the detection of islet amyloid with PET. In this study, we showed that [ $^{18}\text{F}$ ]FDDNP selectively stained the human pancreas islet amyloid. This specific binding was proved by autoradiography. We also evaluated the distribution and the clearance of [ $^{18}\text{F}$ ]FDDNP in healthy humans to confirm that it has favorable pharmacokinetics as a potential islet amyloid PET tracer.

## Patients and methods

### The ethical consideration

The use of patients' tissue and imaging data in this study was approved by the Institute Research Medical Ethics Committee of First Affiliated Hospital of Dalian Medical University. Informed written consent was obtained from all patients before the study.

### General information

Paraffin-embedded human pancreas samples from a T2DM patient (a 69-year-old man) and a healthy individual (a 72-year-old woman) were generously provided by the Department of Pathology, the First Affiliated Hospital of Dalian Medical University, People's Republic of China. The pancreas samples were cut into 3–5 mm thick sections that were either used immediately after deparaffinization or after the antigen retrieval procedure involving 30 min of autoclaving at 121°C in distilled water and subsequent incubation in 96% formic acid for 5 min, which is the standard pretreatment for pancreas islet amyloid immunostain detection [14]. The presence of islet amyloid was determined by two senior pathologists independently.

### Hematoxylin and eosin staining

The dewaxed and hydrated human pancreas tissue sections were incubated with alum haematoxylin solution at room temperature (RT) for 5 min before rinsing with distilled water for 1 min, 1% HCl in ethanol for 20 s, and distilled water for 1 min. The sections were then incubated with 0.5% eosin at RT for 2 min, rinsed with

distilled water for 1 min, dehydrated, and mounted with glycerol before observation under a Nikon Eclipse E600 microscope with a Nikon DXM 1200 digital camera (Nikon, Tokyo, Japan) ( $\times 200$  objective).

### Congo Red staining

The dewaxed and hydrated human pancreas tissue sections were incubated with alum haematoxylin solution at RT for 2 min and then in 0.5% HCl in ethanol for 20 s before rinsing with distilled water twice for 5 min. The sections were then incubated in 1% Congo Red solution at RT for 25 min, rinsed with distilled water for 2 min, dehydrated, and mounted with glycerol before observation under a Nikon Eclipse E600 microscope with a Nikon DXM 1200 digital camera (Nikon) ( $\times 200$  objective).

### Periodic acid-Schiff staining

The dewaxed and hydrated human pancreas tissue sections were incubated in 0.5% periodic acid water solution at RT for 20 min before rinsing with distilled water twice. The sections were then incubated with Schiff reagent at RT for 10 min until the sections became light pink in color and were then washed with distilled water till the sections turned into a dark pink color in 5 min. Subsequently, the sections were incubated with hematoxylin for 2 min and then in 0.5% HCl in ethanol for 10 s before washing with distilled water, dehydrated, and mounted with glycerol before observation under a Nikon Eclipse E600 microscope with a Nikon DXM 1200 digital camera (Nikon) ( $\times 200$  objective).

### Immunohistochemistry

The dewaxed and hydrated human pancreas tissue sections were washed with PBS three times, incubated with normal horse serum 4% in PBS at RT for 20 min, and then the anti-amylin antibody (10  $\mu\text{g}/\text{ml}$ , ab11022; Abcam, Bristol, UK) at 4°C for 18 h. Subsequently, the sections were incubated with maxvision/HRP for 15 min, washed with PBS three times, and rinsed with 3,3'-diaminobenzidine till the color developed. The sections were washed with distilled water and then incubated with hematoxylin for 2 min before washing with distilled water, dehydrated, and mounted with glycerol before observation under a Nikon Eclipse E600 microscope with a Nikon DXM 1200 digital camera (Nikon) ( $\times 200$  objective).

### [ $^{18}\text{F}$ ]FDDNP fluorescence staining

The dewaxed and hydrated human pancreas tissue sections were incubated with 1% Sudan black in a 70% ethanol solution at RT for 5 min and rinsed with distilled water and 70% ethanol. The sections were then incubated in [ $^{18}\text{F}$ ]FDDNP (5  $\mu\text{mol}/\text{l}$ ; ABX company, Radeberg, Germany) in the dark for 30 min, rinsed with distilled water for 2 min, and mounted with glycerol before observation under an EVOS FL Imaging System (Thermo Fisher; Waltham, Massachusetts, USA) ( $\times 200$  objective) with GFP Light Cube [15].

### **[<sup>18</sup>F]FDDNP autoradiography and blocking with its reference compound**

The [<sup>18</sup>F]FDDNP was prepared on the basis of a previously published method [16]. The dewaxed and hydrated human pancreas tissue sections were incubated in [<sup>18</sup>F]FDDNP PBS solution (0.13 MBq/ml) with or without its nonradioactive reference compound (0.44 mg/ml) in the dark for 20 min. The sections were then washed with distilled water and air dried before exposure to a multi-sensitive phosphor screen (PerkinElmer; Waltham, Massachusetts, USA) at RT for 5 min. The phosphor screen was then scanned in a Typhoon 8600 phosphor imager (GE Healthcare; Pittsburgh, Pennsylvania, USA) at a resolution of 50 μm. The images were analyzed using OptiQuant (version 5.0; PerkinElmer) software.

### **[<sup>18</sup>F]FDDNP dynamic pancreas PET/CT imaging**

Four healthy volunteers (Table 1) received [<sup>18</sup>F]FDDNP (370 MBq) and subjected to a pancreatic three-dimensional mode dynamic PET/CT scan (Biograph 64; Siemens AG, Muenchen, Germany) from 5 to 120 min after intravenous injection, respectively. The pancreas was localized by a care-dose (quality reference current 170 mAs, 120 kVp, free tidal breathing) computed tomography (CT) scan. The images were reconstructed using True X with a 168 × 168 matrix size, ordered-subsets expectation maximization (three iterations, 21 subsets, zoom 1), and postfilter full-width at half-maximum of 4 mm. Quantitative image analysis was based on the transaxial frames of [<sup>18</sup>F]FDDNP DICOM series images by drawing the Region of Interest (ROI) with a diameter of 0.8 cm and then measuring the mean standardized uptake values (SUV<sub>mean</sub>) of radioactivity uptake in the whole pancreas including head, neck, body and tail, blood pool (abdominal aorta at the lumbar level L1, L2), liver (right lobe), and vertebral bone. On the DICOM reconstructed images, a ROI standard-sized region with a diameter of 0.8 cm in the center of the abdominal aorta at the lumbar level (L1, L2) was used to measure the blood pool SUVs; and in the whole pancreatic, the right lobe of liver, and vertebral bone in sight.

## **Results**

### **Islet amyloids detected in the human pancreas tissue by H&E staining**

To confirm the presence of islet amyloids in the human pancreas tissue from a T2DM patient (a 69-year-old man),

we stained its section slides with H&E. A large number of islet amyloids were observed as light red clusters in the pancreatic islet indicated by the arrows (Fig. 1a).

### **Islet amyloids' detection by the [<sup>18</sup>F]FDDNP reference compound**

To demonstrate the ability of [<sup>18</sup>F]FDDNP to detect islet amyloids, we stained the consecutive pancreas tissue sections from a T2DM patient (a 69-year-old man) using the standard islet amyloid detecting methods, such as the Congo Red, periodic acid-Schiff (PAS), and anti-amylin antibody, to compare with that of the [<sup>18</sup>F]FDDNP reference compound. The islet amyloids in the pancreas tissue sections were visualized by the Congo Red as orange red clusters, the PAS as pink clusters, and the anti-amylin antibody as brown clusters indicated by the arrows under bright-field microscopy (Fig. 1b–d). The islet amyloids were also detected by the [<sup>18</sup>F]FDDNP reference compound as bright yellow clusters with fluorescence imaging (Fig. 1e). In contrast, when healthy human pancreas tissue sections (a 72-year-old woman) were incubated with the [<sup>18</sup>F]FDDNP reference compound, little [<sup>18</sup>F]FDDNP residual was retained in the tissue after washing with water (Fig. 1f).

### **[<sup>18</sup>F]FDDNP binding to islet amyloids in human pancreas tissue sections**

The [<sup>18</sup>F]FDDNP was prepared using an Explora GN modular lab (Siemens AG; Muenchen, Germany) in nondecay correct isolated radiochemical yields of 10.4 ± 1.8% (*n* = 5) with a radiochemical purity of more than 99% with a specific activity of 86 GBq/μmol using an established literature method [16]. We investigated the selectivity and specificity of [<sup>18</sup>F]FDDNP to bind to islet amyloids in human pancreas tissue sections using an autoradiograph. The dewaxed and hydrated human pancreas tissue sections from a T2DM patient (a 69-year-old man) were incubated in an [<sup>18</sup>F]FDDNP PBS solution with or without its reference compound in the dark before exposure to a multisensitive phosphor screen. The phosphor screen was then scanned in a Typhoon 8600 phosphor imager. The autoradiograph images showed that [<sup>18</sup>F]FDDNP accumulated in the islet amyloids as dots and patches in the human pancreas tissue sections (Fig. 2a and c). The specific uptake of these islet amyloids was largely blocked by the FDDNP reference compound in the continuous tissue section (Fig. 2b and c).

### **[<sup>18</sup>F]FDDNP rapidly cleared from pancreas in controls without T2DM**

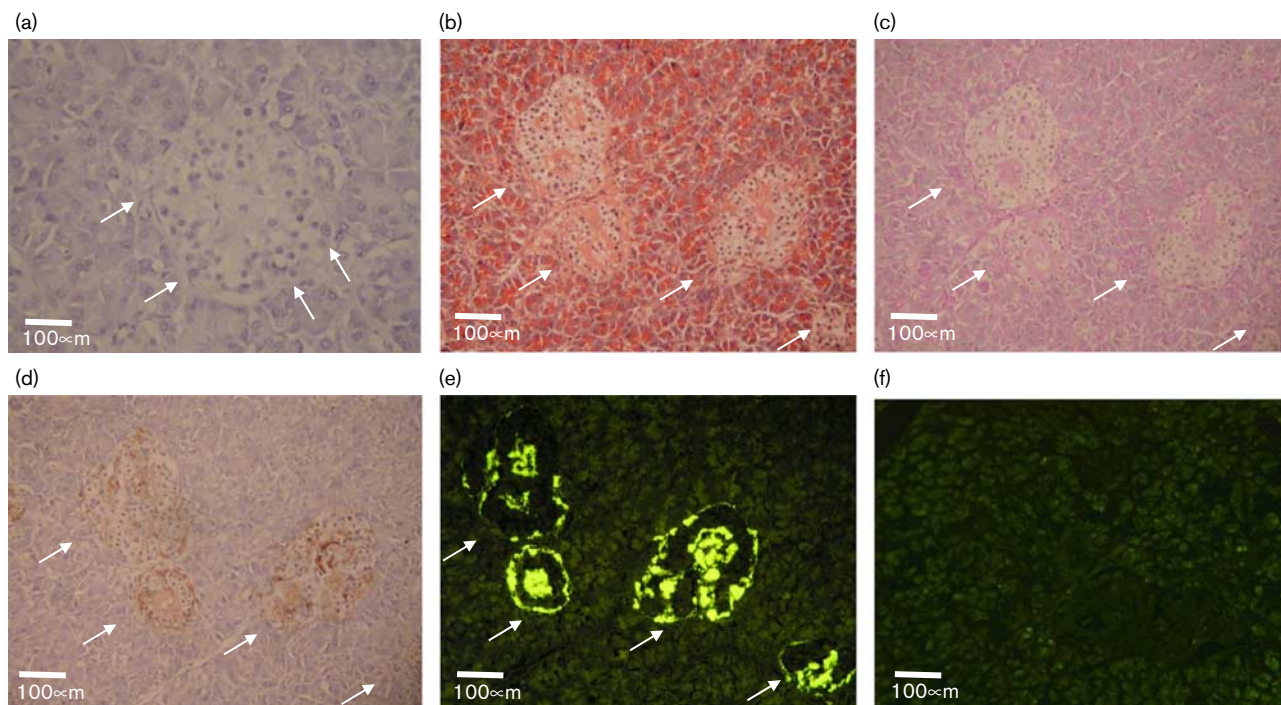
Four individuals without T2DM who had received [<sup>18</sup>F]FDDNP were subjected to pancreatic three-dimensional mode dynamic PET/CT scans from 5 to 120 min after an intravenous injection, respectively. The pancreas was localized by a care-dose CT scan. To quantify the radioactivity uptake in the entire pancreas including the head, neck, body, and tail, blood pool, liver, and vertebral

**Table 1** Characteristics of human participants in the PET study

Patients	Age (years)	Sex	Pancreas disease	T2DM	Fasting blood glucose level (mmol/l)
1	29	Female	No	No	5.0
2	53	Female	No	No	6.0
3	63	Female	No	No	4.6
4	60	Male	No	No	5.7

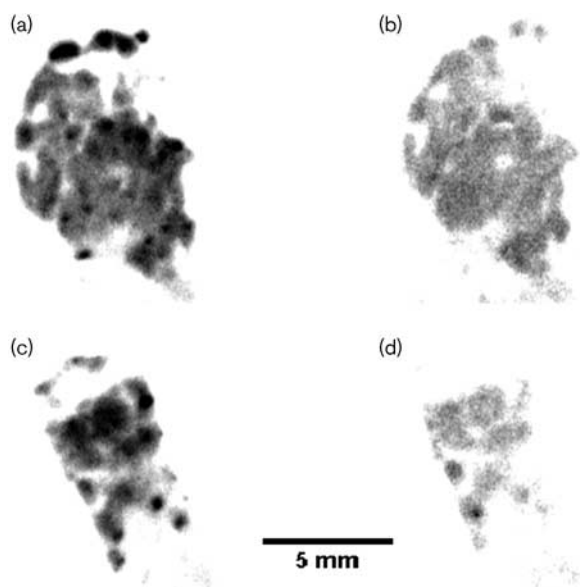
T2DM, type 2 diabetes mellitus.

**Fig. 1**



(a) H&E staining of a T2DM patient's pancreas tissue section; (b–d) continuous pancreas tissue sections staining from the same T2DM patients' pancreas tissue: (b) Congo Red; (c) PAS; (d) anti-amylin antibody IHC staining; (e) fluorescence from FDDNP; (f) FDDNP staining with a human pancreas tissue section without T2DM. The white arrows in (a–e) indicate the locations of the amyloid in the pancreas tissue sections.

**Fig. 2**



(a–d) Autoradiography of a type 2 diabetes mellitus patient's pancreas tissue sections. (a, c) incubated with  $[^{18}\text{F}]\text{FDDNP}$  alone; (b, d) incubated with  $[^{18}\text{F}]\text{FDDNP}$  in the presence of its nonradioactive reference compound.

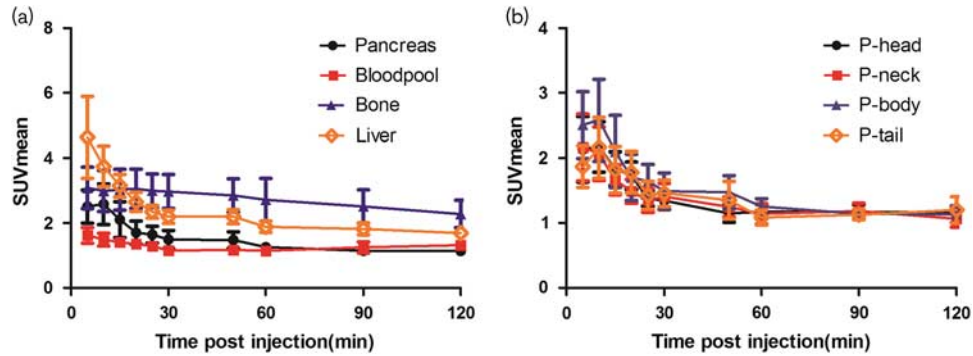
bone, the  $\text{SUV}_{\text{mean}}$  were determined by drawing the ROI on the transaxial frames of  $[^{18}\text{F}]\text{FDDNP}$  series images. The mean SUVs of the pancreas were decreased to close to the blood pool level 30 min post intravenous injection (Fig. 3a). Furthermore, the pancreatic head, neck, body, and tail had similar  $[^{18}\text{F}]\text{FDDNP}$  uptake throughout the PET scan, showing an initial increased uptake in the first 5 min, gradually decreasing till 60 min, and reaching a plateau from 60 to 120 min (Fig. 3b). Moreover, in the transaxial PET images of  $[^{18}\text{F}]\text{FDDNP}$  PET/CT scan of the control human participant (Fig. 4), the pancreas could be clearly visualized and distinguished from the liver and other metabolism organs at all-time points from 5 to 120 min despite the fact that the  $\text{SUV}_{\text{mean}}$  from the liver and bone were slightly higher than those in the pancreas. Gradual radioactivity accumulation and excretion in the gallbladder, the bright spot close to the pancreatic head, was also observed from the PET images in Fig. 4.

### Discussion

There are strong evidences that T2DM and AD are closely associated protein misfolding disorders and the islet and AD  $\beta$ -amyloid shares similar secondary structures [11,12]. Thus, an AD PET tracer such as  $[^{18}\text{F}]\text{FDDNP}$  could be

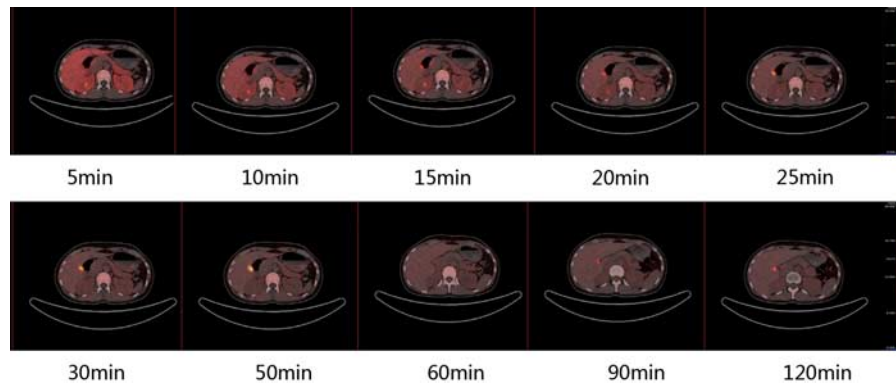


Fig. 3



(a) The mean standardized uptake value (SUV<sub>mean</sub>) of radioactivity retention in the pancreas, blood pool, liver, and bone in the controls. (b) The SUV<sub>mean</sub> of radioactivity retention in the pancreatic head, neck, body, and tail, respectively, in the controls.

Fig. 4



The representative transaxial frames of the [<sup>18</sup>F]FDDNP PET/CT scan of the pancreas and the neighboring organs in a control human participant at different time points from 5 to 120 min after an intravenous injection.

used for the noninvasive imaging of islet amyloid in T2DM patients. We investigated its suitability to detect islet amyloids in humans with the added advantage that it could measure the amyloid burden in both the central nervous system and the peripheral organs at the same time, which might unveil the interrelationship of these two age-related diseases at the molecular level.

Initially, we confirmed the presence of islet amyloids in the human pancreas tissue from a T2DM patient (a 69-year-old man) using the H&E histology method. The islet amyloids were observed as light red clusters and distributed heterogeneously in this pancreas specimen. In the subsequent comparison staining study, we observed the islet amyloids as bright yellow clusters stained by the [<sup>18</sup>F]FDDNP reference compound with fluorescence imaging. These islet amyloids have distributions and phenotypes similar to those in the continues human pancreas tissue sections detected by the standard islet amyloid staining methods using Congo

Red, PAS, and anti-amylin antibody. In the control experiment, [<sup>18</sup>F]FDDNP was not retained in the healthy human pancreas tissue. These data gave us the confidence that FDDNP can be used to detect islet amyloids. To further confirm that the binding between [<sup>18</sup>F]FDDNP and the islet amyloids is selective and specific at the tracer level, we incubated the islet amyloid containing human pancreas tissue sections in the [<sup>18</sup>F]FDDNP PBS solution with and without the addition of its cold reference compound. Selective accumulation of [<sup>18</sup>F]FDDNP in the islet amyloid-enriched regions was observed in the autoradiography. The specific binding of [<sup>18</sup>F]FDDNP to the islet amyloid was confirmed by the fact that most of the [<sup>18</sup>F]FDDNP accumulation was blocked by its reference compound.

As a small lipophilic molecule, [<sup>18</sup>F]FDDNP would show high uptake in the liver, which could make it difficult to visualize islet amyloid deposits in the pancreas. Thus, before testing [<sup>18</sup>F]FDDNP on the T2DM patients, we

investigated its distribution and clearance in healthy human volunteers. The distribution of radioactivity in the pancreas from 5 to 120 min after an intravenous injection was very low and could be distinguished easily from other neighboring organs including the liver, bone, kidney, and stomach. The  $SUV_{mean}$  in the pancreas became very close to the blood pool level after 30 min. In addition, the different parts of the pancreas such as the head, neck, body, and tail had similar low [ $^{18}F$ ]FDDNP uptake during the PET scan. All these characteristics generate a low background, which is essential to visualize islet amyloids in the entire pancreas in the T2DM patients. We believe that targeting the islet amyloidosis for the assessment of pancreatic  $\beta$ -cell function in T2DM patients rather than the direct quantification of pancreatic  $\beta$ -cell mass provides an attractive alternative strategy as the latter approach has been proven to be very challenging [17]. Thus, [ $^{18}F$ ]FDDNP shows suitable in-vitro selectivity and specificity, and in-vivo pharmacokinetics was found to be a promising islet amyloids PET tracer.

## Conclusion

We have systematically investigated the suitability of [ $^{18}F$ ]FDDNP as a PET tracer to detect pancreatic islet amyloid. Both the [ $^{18}F$ ]FDDNP reference compound and the [ $^{18}F$ ]FDDNP can selectively and specifically target the islet amyloid in human pancreas tissue. [ $^{18}F$ ]FDDNP has low uptake and cleared rapidly from the pancreas, blood pool, and liver in the healthy human participants, which generated a low background to image the islet amyloid. A clinical trial that aims to measure the pancreatic islet amyloid burden in T2DM patients using [ $^{18}F$ ]FDDNP is currently ongoing.

## Acknowledgements

The authors would like to thank the Scientific Research Project for Institutes of Higher Education, Ministry of Education, Liaoning Province (L2015149), China, for supporting this work. The research undertaken at King's College London was funded by the National Institute for Health Research (NIHR) Biomedical Research Centre based at Guy's and St Thomas' NHS Foundation Trust and King's College London, the Wellcome/EPSCRC Centre for Medical Engineering at King's College London (WT 203148/Z/16/Z), the King's College London, and the UCL Comprehensive Cancer Imaging Centre funded by CRUK and EPSRC in association with the MRC and DoH (UK).

## Conflicts of interest

There are no conflicts of interest.

## References

- 1 WHO. Global report on diabetes, World Health Organization; 2016 WHO/NMH/NVI/16.3. Available at: <http://www.who.int/diabetes/global-report>. [Accessed 8 August 2017].
- 2 Johnson KH, O'Brien TD, Betsholtz C, Westermarck P. Islet amyloid, islet-amyloid polypeptide, and diabetes mellitus. *N Engl J Med* 1989; **24**:513–518.
- 3 Röcken C, Linke RP, Saeger W. Immunohistology of islet amyloid polypeptide in diabetes mellitus: semi-quantitative studies in a post-mortem series. *Virchows Arch A Pathol Anat Histopathol* 1992; **421**:339–344.
- 4 Cooper GJ, Willis AC, Clark A, Turner RC, Sim RB, Reid KB. Purification and characterization of a peptide from amyloid-rich pancreases of type 2 diabetic patients. *Proc Natl Acad Sci* 1987; **84**:8628–8632.
- 5 Kahn SE, Andrikopoulos S, Verchere CB. Islet amyloid: a long-recognized but underappreciated pathological feature of type 2 diabetes. *Diabetes* 1999; **48**:241–253.
- 6 Wang F, Hull RL, Vidal J, Cnop M, Kahn SE. Islet amyloid develops diffusely throughout the pancreas before becoming severe and replacing endocrine cells. *Diabetes* 2001; **50**:2514–2520.
- 7 Howard CF Jr. Longitudinal studies on the development of diabetes in individual *Macaca nigra*. *Diabetologia* 1986; **29**:301–306.
- 8 Howard CF Jr, Van Bueren A. Changes in islet cell composition during development of diabetes in *Macaca nigra*. *Diabetes* 1986; **35**:165–171.
- 9 De Koning EJ, Bodkin NL, Hansen BC, Clark A. Diabetes mellitus in *Macaca mulatta* monkeys is characterised by islet amyloidosis and reduction in beta-cell population. *Diabetologia* 1993; **36**:378–384.
- 10 Yoshimura M, Ono M, Watanabe H, Kimura H, Saji H. Development of (99m)Tc-labeled pyridyl benzofuran derivatives to detect pancreatic amylin in islet amyloid model mice. *Bioconjug Chem* 2016; **15**:1532–1539.
- 11 Agdeppa ED, Kepe V, Liu J, Flores-Torres S, Satyamurthy N, Petric A, et al. Binding characteristics of radiofluorinated 6-dialkylamino-2-naphthylethylidene derivatives as positron emission tomography imaging probes for beta-amyloid plaques in Alzheimer's disease. *J Neurosci* 2001; **21**:RC189.
- 12 Shoghi-Jadid K, Small GW, Agdeppa ED, Kepe V, Ercoli LM, Siddarth P, et al. Localization of neurofibrillary tangles and beta-amyloid plaques in the brains of living patients with Alzheimer disease. *Am J Geriatr Psychiatry* 2002; **10**:24–35.
- 13 Blázquez E, Velázquez E, Hurtado-Carneiro V, Ruiz-Albusac JM. Insulin in the brain: its pathophysiological implications for States related with central insulin resistance, type 2 diabetes and Alzheimer's disease. *Front Endocrinol (Lausanne)* 2014; **5**:1–21.
- 14 Schnell SA, Staines WA, Wessendorf MW. Reduction of lipofuscin-like autofluorescence in fluorescently labeled tissue. *J Histochem Cytochem* 1999; **47**:719–730.
- 15 Bresjanac M, Smid LM, Vovko TD, Petric A, Barrio JR, Popovic M. Molecular-imaging probe 2-(1-[6-[(2-fluoroethyl)(methyl)amino]-2-naphthyl]ethylidene) malononitrile labels prion plaques in vitro. *J Neurosci* 2003; **23**:8029–8033.
- 16 Liu J, Kepe V, Zabjek A, Petric A, Padgett HC, Satyamurthy N, Barrio JR. High-yield, automated radiosynthesis of 2-(1-[6-[(2- $^{18}F$ fluoroethyl)(methyl)amino]-2-naphthyl]ethylidene) malononitrile ([ $^{18}F$ ]FDDNP) ready for animal or human administration. *Mol Imaging Biol* 2007; **9**:6–16.
- 17 Wängler B, Schneider S, Thews O, Schirmacher E, Comagic S, Feilen P, et al. Synthesis and evaluation of (S)-2-(2-[ $^{18}F$ ]fluoroethoxy)-4-[[3-methyl-1-(2-piperidin-1-yl-phenyl)-butyl-carbamoyl]-methyl]-benzoic acid ([ $^{18}F$ ]repaglinide): a promising radioligand for quantification of pancreatic beta-cell mass with positron emission tomography (PET). *Nucl Med Biol* 2004; **31**:639–647.